Molecular Therapy
Methods & Clinical Development
Original Article

Improved diabetic wound healing by LFcinB is associated with relevant changes in the skin immune response and microbiota

Michelle V. Mouritzen,[1,6] Marija Petkovic,[1,2,3,6] Katrine Qvist,[1] Steen S. Poulsen,[4] Susana Alarico,[2,3] Ermelindo C. Leal,[2,3] Louise T. Dalgaard,[1] Nuno Empadinhas,[2,3] Eugenia Carvalho,[2,3,5] and Håvard Jenssen[1]

[1]Department of Science and Environment, Roskilde University, Roskilde, Denmark; [2]Center for Neuroscience and Cell Biology, University of Coimbra, Coimbra, Portugal; [3]Institute for Interdisciplinary Research, University of Coimbra, Coimbra, Portugal; [4]Department of Biomedical Science, University of Copenhagen, Copenhagen, Denmark; [5]Department of Geriatrics, University of Arkansas for Medical Sciences, and Arkansas Children's Research Institute, Little Rock, AR, USA

Bovine lactoferricin (LFcinB) has antimicrobial and immunomodulatory properties; however, the effects on diabetic wound healing remain poorly understood. The wound healing potential of LFcinB was investigated with *in vitro*, *ex vivo*, and *in vivo* models. Cell migration and proliferation were tested on keratinocytes and on porcine ears. A type 1 diabetic mouse model was also used to evaluate wound healing kinetics, bacterial diversity patterns, and the effect of LFcinB on oxidative stress, macrophage phenotype, angiogenesis, and collagen deposition. LFcinB increased keratinocyte migration *in vitro* ($p < 0.05$) and *ex vivo* ($p < 0.001$) and improved wound healing in diabetic mice ($p < 0.05$), though not in normoglycemic control mice. In diabetic mouse wounds, LFcinB treatment led to the eradication of *Bacillus pumilus*, a decrease in *Staphylococcus aureus*, and an increase in the *Staphylococcus xylosus* prevalence. LFcinB increased angiogenesis in diabetic mice ($p < 0.01$), but this was decreased in control mice ($p < 0.05$). LFcinB improved collagen deposition in both diabetic and control mice ($p < 0.05$). Both oxidative stress and the M1-to-M2 macrophage ratios were decreased in LFcinB-treated wounds of diabetic animals ($p < 0.001$ and $p < 0.05$, respectively) compared with saline, suggesting a downregulation of inflammation in diabetic wounds. In conclusion, LFcinB treatment demonstrated noticeable positive effects on diabetic wound healing.

INTRODUCTION

Chronic non-healing wounds constitute an increasing problem worldwide. Macrovascular and microvascular complications of long-standing diabetes result in neuropathy and lower limb ischemia that are critical risk factors for chronic non-healing wounds.[1] Non-healing wounds are a frequent late-diabetic complication and a major reason for lower limb amputations.[2] Cellular characteristics of diabetic wounds include impairments in keratinocyte function and angiogenesis as well as chronic low-grade inflammation.[3] Normal wound healing is separated into four overlapping phases: (1) inflammation, (2) proliferation, (3) migration, and (4) remodeling. Diabetic wounds become stalled in the inflammatory phase, resulting in an accumulation of immune cells at the wound site, increased reactive oxygen species (ROS) generation, and an increase in pro-inflammatory cytokines.[4] Altogether, this destructive micro-environment impairs angiogenesis and thereby formation of healthy granulate tissue, which in turn inhibits re-epithelialization.[5] When wounds fail to close, opportunistic pathogens colonize the wound site and drive biofilm formation, influencing recruitment of host immune cells.[6] This leads to a negative impact on recovery by maintaining the wound in a prolonged inflammatory phase, further impairing the healing process. An ideal candidate for treating the non-healing wounds in diabetic patients should therefore control pathogen infection, improve the microenvironment, and promote continued healing.

Lactoferrin (LF) is a protein found in various secretory fluids including milk of various mammals, including humans. Interestingly, it has activity against bacteria,[7] viruses,[8] fungi,[9] and cancer cells.[10] Additionally, LF also affects migration, proliferation,[11] and expression of pro-inflammatory cytokine.[12] Furthermore, a recombinant form of the human LF (hLF), talactoferrin, was demonstrated to improve wound healing *in vivo* in a murine model.[13]

From the protein bovine LF (bLF), a small peptide of 25 amino acids (aa), called bovine lactoferricin (LFcinB), has also been found to confer antimicrobial activity.[14] The activity of LFcinB was confirmed against both Gram-positive and Gram-negative bacteria, and, interestingly, LFcinB showed an increased or similar effect as bLF.[15] Moreover, LFcinB has immunomodulatory properties demonstrated by its ability to bind endotoxin.[16,17] Together, this makes LFcinB a good potential therapeutic candidate for diabetic wounds against infection, boosting the wound microenvironment, and promoting continued healing.

Received 28 September 2020; accepted 5 February 2021;
https://doi.org/10.1016/j.omtm.2021.02.008.

[6]These authors contributed equally

Correspondence: Håvard Jenssen, Department of Science and Environment, Roskilde University, Universitetsvej 1, 28A.2, 4000 Roskilde, Denmark.
E-mail: jenssen@ruc.dk

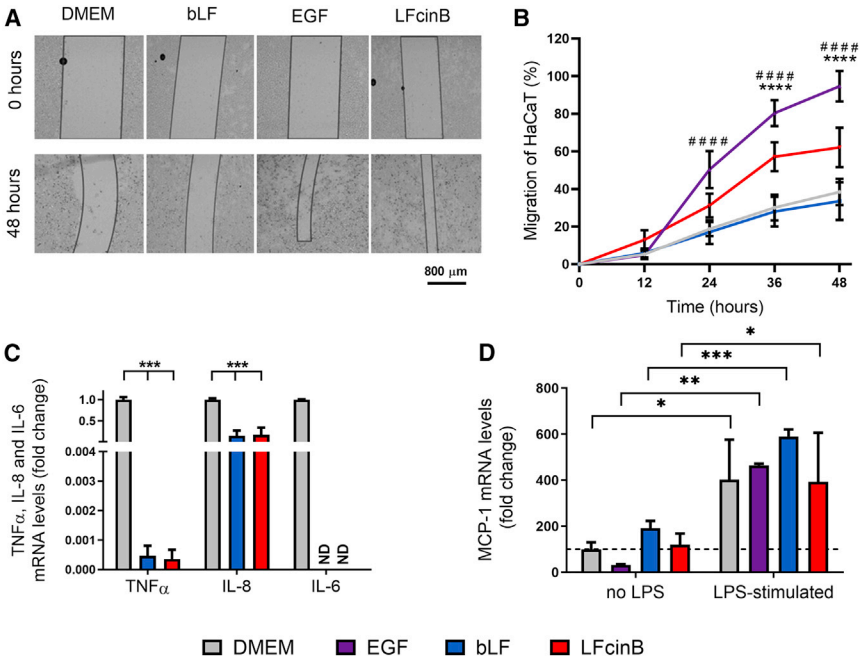

Figure 1. Lactoferricin (LFcinB) and bovine lactoferrin (bLF) increase HaCaT cell migration *in vitro* and decrease LPS-stimulated cytokine mRNA transcript levels

(A) Representative images of HaCaT cell re-epithelialization at time 0 and 48 h post-scratch. The migratory potential of LFcinB was evaluated on an oCelloScope. The cells were treated with LFcinB, bLF, epidermal growth factor (EGF), and DMEM (cell culture medium). The scratched area (non-cell area) is marked with black lines to distinguish the boundaries between the gap and the cell-covered area. (B) Quantification of HaCaT cell migration. The effects of treatments with EGF, bLF, or LFcinB on cell migration rate were compared with the untreated cells and shown as percentage of migrated cells at time points 0, 12, 24, 36, and 48 h. (C) LPS-stimulated (10 ng/mL) mRNA expression levels of tumor necrosis factor-α (TNF-α), interleukin-6 (IL-6), and IL-8 in HaCaT cells after 24 h treatment with LFcinB or bLF. The mRNA level of IL-6 was not detectable (ND) after LFcinB or bLF treatments. (D) Expression levels of monocyte chemoattractant protein 1 (MCP-1) from HaCaT cells after 24 h treatment with LFcinB, EGF, or DMEM, with or without LPS (10 ng/mL). The data represent normalized levels. (B–D) Mean ± SD of 3 independent experiments performed in triplicate, comparing the difference between (B) EGF (#) and LFcinB (*) and DMEM; (C) bLF and LFcinB and DMEM; and (D) DMEM, bLF, EGF, and LFcinB non-treated cells and LPS stimulated (*). *$p < 0.05$, **$p < 0.01$, ***$p < 0.001$, ****,####$p < 0.0001$.

Here, we compared the effects of LFcinB with those of the full-length bLF protein using *in vitro* cellular migration and gene-expression assays. We further characterized the effect of LFcinB with an *ex vivo* wound healing model as well as an *in vivo* full-thickness wound model comparing control and diabetic mice.

RESULTS

LFcinB enhances keratinocyte migration *in vitro* and decreases cytokine expression

The migratory effect of LFcinB and the full-length bLF was investigated in an immortalized keratinocyte cell line (HaCaT) (Figure 1A). The oCelloScope was set to record the migration for 48 h and to acquire images every 12th hour (Figure 1B). After 24 h, a significant increase in migration was demonstrated for LFcinB (31% ± 6% of scratch width, $p < 0.05$) and epidermal growth factor (EGF) (50% ± 10%, $p < 0.0001$) compared with the control (19% ± 4%). EGF is a mitogen that affects migration of proliferation of cells and enhances wound healing.[18] Surprisingly, there were no significant effects of full-length bLF on migration (17% ± 6%, not significant [NS]). Similarly, 48 h LFcinB (62% ± 10%, $p < 0.001$) and EGF (95% ± 8%, $p < 0.001$) treatment significantly enhanced migration compared with the control (38% ± 7%), while no effect of bLF on migration was observed (34% ± 10%, NS).

The proliferative effects of LFcinB and bLF were also investigated in HaCaT cells. While EGF significantly increased proliferation (by 78% ± 6%, $p < 0.05$), neither LFcinB (69% ± 13%, NS) nor bLF (70% ± 16%, NS) increased the amount of HaCaT cells compared with the control (59% ± 4%) (Figure S1). Since LFcinB significantly enhanced migration at 24 h post-scratching compared with the control, using the *in vitro* scratch assay, the 24 h time point was chosen for quantification of mRNA expression of the key pro-inflammatory cytokines tumor necrosis factor (TNF)-α, interleukin (IL)-6, and IL-8 to investigate the immunomodulatory effects of LFcinB and bLF following lipopolysaccharide (LPS) treatment (Figure 1C). Treatment with LFcinB and bLF inhibited mRNA levels of TNF-α and IL-8: TNF-α by LFcinB (0.0036 ± 0.00032, $p < 0.001$) and by bLF (0.0047 ± 0.00034, $p < 0.001$) and IL-8 by LFcinB (0.17 ± 0.16, $p < 0.001$) and by bLF (0.15 ± 0.12, $p < 0.001$) relative to the control (Figure 1C). Interestingly, the mRNA levels of IL-6 were not detectable (ND) post-treatment for either LFcinB or bLF, while robustly present in the control (Figure 1C).

We investigated whether LFcinB and bLF influenced the secretion of monocyte chemoattractant protein 1 (MCP-1) from HaCaT cells (Figure 1D). Treatment with LFcinB did not significantly increase MCP-1 levels (120% ± 49%, NS) compared with the control (100% ± 31%), whereas bLF increased MCP-1 levels (192% ± 32%, NS). When HaCaT cells were stimulated with LPS, levels of MCP-1 were significantly increased (403% ± 173%, $p < 0.05$) compared with the untreated control. This was expected, as LPS activates transcription factors that promote production of pro-inflammatory

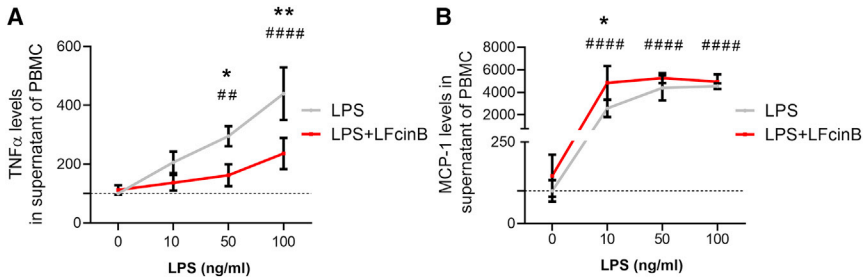

Figure 2. Secreted cytokine levels from human peripheral blood mononuclear cells (PBMCs) after treatments with LFcinB and LPS

PBMCs isolated from healthy donors were treated with LFcinB (25 μg/mL) or LPS (10, 50, or 100 ng/mL) for 24 h and investigated by ELISA. (A) Secreted levels of TNF-α. (B) Secreted levels of MCP-1. The graphs show the mean ± SD for 3 independent donors in triplicate, comparing the difference between the LFcinB and DMEM LPS (10 ng/mL)-treated and non-treated cells (*) and LPS response in a dose-dependent manner compared with non-treated cells (#). $^{*}p < 0.05$, $^{**,\#\#}p < 0.01$, $^{\#\#\#\#}p < 0.0001$.

factors.[19] Co-stimulation with LPS and LFcinB led to increased levels of MCP-1 compared with untreated control (392% ± 212%, $p < 0.05$). Likewise, co-stimulation with LPS and bLF (509% ± 31%, $p < 0.001$) increased MCP-1 levels compared with untreated cells. However, LFcinB was not able to diminish the LPS-induced increase in MCP-1 secretion from HaCaT cells (394% ± 212%, NS) compared with LPS-only treated cells (120% ± 49%).

The impact of LFcinB on MCP-1 and TNF-α levels was also investigated in peripheral blood mononuclear cells (PBMCs) isolated from healthy donors. PBMCs were treated with LFcinB, LPS, or medium alone (control). LPS was used at increasing concentrations (10, 50, and 100 ng/mL) alone or in combination with LFcinB. LPS alone caused a dose-dependent increase of 2-fold with 50 ng/mL LPS (206% ± 36%, $p < 0.01$) to 4-fold with 100 ng/mL LPS (440% ± 90%, $p < 0.001$) of TNF-α levels secreted from PBMCs into the culture medium from untreated control (100% ± 4%). (Figure 2A). However, when PBMCs were co-stimulated with LFcinB and 50 ng/mL or 100 ng/mL of LPS, the TNF-α levels secreted from PBMCs were withdrawn almost 2-fold for both concentrations (162% ± 37%, $p < 0.05$ and 236% ± 53%, $p < 0.01$, respectively) compared with 50 ng/mL and 100 ng/mL LPS stimulation only.

PBMCs were also used to measure the levels of MCP-1, with LPS (10, 50, and 100 ng/mL) and LFcinB co-stimulated with LPS and without LPS (Figure 2B). LPS alone in media led to a 500-fold increase in MCP-1 levels for all the tested concentrations ($p < 0.0001$). Co-stimulation in human PBMCs showed responsiveness to 10 ng/mL LPS and LFcinB treatment by increasing MCP-1 secretion 2-fold (4,833% ± 1,510%, $p < 0.05$) compared with 10 ng/mL of LPS only (2,567% ± 779%).

Enhanced migration and proliferation in a porcine *ex vivo* wound healing model

Porcine skin has similarities to human skin with respect to fat composition, epidermal thickness, and dermal-to-epidermal thickness ratios[20] as well as location and identity of immune cells.[21] Together, these features make porcine skin an attractive model for wound healing.[22] We treated wounded porcine ear skin *ex vivo* with LFcinB, conventional medium (Dulbecco's modified Eagle's medium [DMEM]), or free aa in the same molar ratio as LFcinB for 5 consecutive days. The aa control was added because free aa are a high-energy source and because they have previously been shown to affect wound healing.[23] Samples were collected for histological analysis at days 1, 3, and 5 post-wounding (Figure 3A) to evaluate epithelial closure (Figure 3B) and cell proliferation (Figure 3C).

After day 1 of treatment, the DMEM control presented a wound closure of 23 ± 7% and 7% ± 8 Ki67-positive epithelial cells/μm^2 (Figures 3A and 3B), which was not different for the LFcinB-treated (31% ± 5%, 10 ± 6 Ki67-positive cells/μm^2, NS) or aa control (29% ± 8%, 8 ± 10 Ki67-positive cells/μm^2) wounds. Interestingly, at day 3, while the epithelial closure for the media treatment had increased to 53 ± 30% (24 ± 24 Ki67-positive cells/μm^2), the LFcinB-treated wounds had reached an epithelial closure of 80 ± 27% ($p < 0.01$) (23 ± 22 Ki67-positive cells/μm^2, NS), which was also increased compared with the aa control (48% ± 23% closure, 12 ± 14 Ki67-positive cells/μm^2, NS) (Figure 3B). Furthermore, at day 5 the epithelial closure of the LFcinB-treated *ex vivo* wound had reached almost complete epithelial closure (95% ± 12%, $p < 0.001$), being significantly increased compared with the DMEM control (82 ± 32%) or the aa control (72% ± 24%) (Figure 3B). Staining for Ki67-positive cells indicated low levels of cell proliferation until day 5 for LFcinB (132 ± 85 Ki67-positive cells/μm^2), while cell proliferation was significantly lower in the DMEM control (70 ± 47 Ki67-positive cells/μm^2) as well as in the aa control (36 ± 25 Ki67-positive cells/μm^2, NS) (Figure 3C).

LFcinB improves wound healing in a mouse model of type 1 diabetes and modulates wound bacterial diversity

To investigate the effect of LFcinB on wound healing *in vivo*, we applied the LFcinB peptide topically to full-thickness excisional wounds in a type 1 diabetes mouse model as well as in non-diabetic control mice. Two different peptide doses were used (12.5 and 25 μg/wound) (Figure 4). In diabetic mice, LFcinB treatment consistently accelerated wound closure, specifically at days 5 and 7–9, compared with the saline treatment for both doses ($p < 0.05$). However, in non-diabetic mice, the low dose of LFcinB inhibited wound healing significantly at days 4–5 ($p < 0.05$) (Figures 4A and 4B).

To analyze the modulatory effect of LFcinB on aerobic resident microbiota, we cultured, isolated, and identified bacteria from swabs from

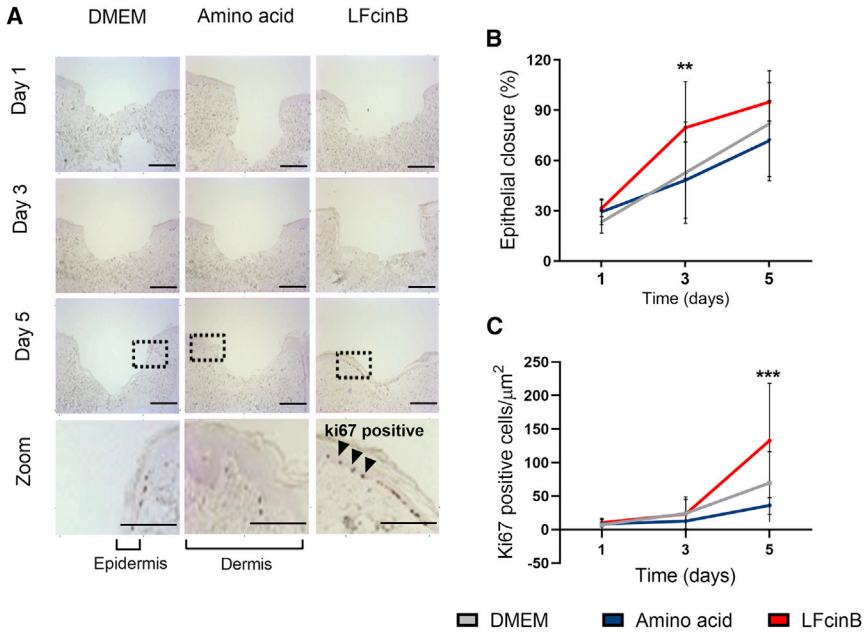

Figure 3. Treatment with LFcinB increases migration and proliferation in an *ex vivo* porcine wound healing model

Ears from freshly slaughtered pigs were cleaned, wounded, and sampled into a 12-well plate with sterile gauze. The skin samples were treated with LFcinB, free amino acids, or DMEM every day for 5 continuous days. Samples were collected at days 0, 1, 3, and 5 for histological analysis of cell migration and proliferation. (A) Representative images after Ki67 staining. The zoom shows a clear separation of the epithelium and dermis layers, where the Ki67-positive cells are located in the epithelial layer. Scale bars, 200 μm and 400 μm. (B) Quantification of epithelial closure calculated as percentage of closure compared to the size of the wound bed. (C) Quantification of Ki67-positive cells in the epithelial layer of the wound bed. The graphs demonstrate the mean ± SD of 2 independent experiments performed in 8 replicates of each treatment for each collection day. **$p < 0.01$, ***$p < 0.001$.

the wound bed at days 0, 5, and 10. The overall community composition analysis at the phylum and genus levels showed a higher diversity of bacterial strains cultivated from diabetic mice compared with non-diabetic mice (Figures 4C and 4D). Most of the species recovered from the swabs belonged to the *Staphylococcus* genus, one of the most common bacterial groups colonizing skin and wounds. Treatment of diabetic wounds with LFcinB promoted an apparent reduction in bacterial diversity compared with saline treatment. From non-diabetic mice, strains of only three major bacterial populations were identified on the skin before wounding. At days 5 and 10, only *E. coli* was identified in all LFcinB-treated samples, while an unidentified strain was observed for the saline treatment. The *E. coli* was not expected to be eradicated, as the minimal inhibition concentration (MIC) for the strain has been reported to be 64 μg/mL.[24] A higher concentration would therefore be necessary to eradicate the species from the wound. For the diabetic mice eight different bacterial strains were identified at day 0, and one was unidentifiable. Treatment with LFcinB decreased strain diversity in the wounds for both concentrations (Figure 4C), and *B. pumilus* completely disappeared after LFcinB treatment. *S. aureus* levels seemed to decrease after treatment with both concentrations of LFcinB (day 5), an observation that seemed to be more pronounced at day 10 for the lowest LFcinB concentration (Figure 4C). Concomitantly, LFcinB treatment led to an increase in levels of commensal *S. xylosus* (day 5) and of *S. epidermidis* (day 10), which suggests that the effect of LFcinB may also involve an antimicrobial activity against the *Staphylococcus* spp. and a stimulating effect on the commensal species.

Anti-inflammatory properties of LFcinB in diabetic wounds

Histological analysis shows that treatment with LFcinB leads to a lower abundance of inflammatory cells in diabetic skin compared with healthy skin. These results agree with the wound healing kinetics results, indicating that diabetic wounds treated with LFcinB heal faster because of lower inflammation at the wound site and at the peri-wound area, with the presence of infiltrate highly enriched in migrating fibroblasts and macrophages (Figure S2). Furthermore, using TNF-α as the M1 macrophage marker and CD206 as the M2 macrophage marker, we investigated macrophage polarization toward the pro-inflammatory or the anti-inflammatory phenotype. We evaluated M1 (Figures 5A and 5E) and M2 (Figures 5A and 5F) macrophage numbers in skin wounds from diabetic mice and from healthy controls (Figures 5B and 5G) as well as the ratio between M1 and M2 macrophages in diabetic mouse (Figure 5I) and non-diabetic mouse (Figure 5K) skin wound biopsies harvested 10 days after excisional wounding. In diabetic wounds, there was no difference in the numbers of pro-inflammatory M1 macrophages between LFcinB- and saline-treated wounds (NS) (Figure 5E), while the number of M2 macrophages was increased by low (8.5 ± 2.6 cells/field, $p < 0.05$), or high (8.7 ± 1.5 cells/field, $p < 0.05$) LFcinB dose compared with the saline treatment (4.7 ± 0.8 cells/field) (Figure 5E). Accordingly, the M1/M2 ratio was decreased 2.1-fold (0.6 ± 0.2 cells/field, $p < 0.05$) and 2.3-fold (0.5 ± 0.2 cells/field, $p < 0.05$) after treatment with low and high doses of LFcinB compared with saline (1.2 ± 0.3 cells/field), respectively (Figure 5I). This indicates an anti-inflammatory effect of LFcinB in diabetic skin wounds. On the other hand, healthy wounds presented decreased M1 macrophages for the high LFcinB dose treatment (10.3 ± 1.9 cells/field, $p < 0.01$) compared with saline (20.6 ± 4.9 cells/field) and M2 macrophages (3.1 ± 0.4 cells/field, $p < 0.01$) compared to saline (4.6 ± 0.2 cells/field). The differences between the two macrophage phenotypes were also found between the high and the low treatment doses, with a significantly increased number of M1 with the low dose (18.8 ± 1. 9 cells/field, $p < 0.05$) compared

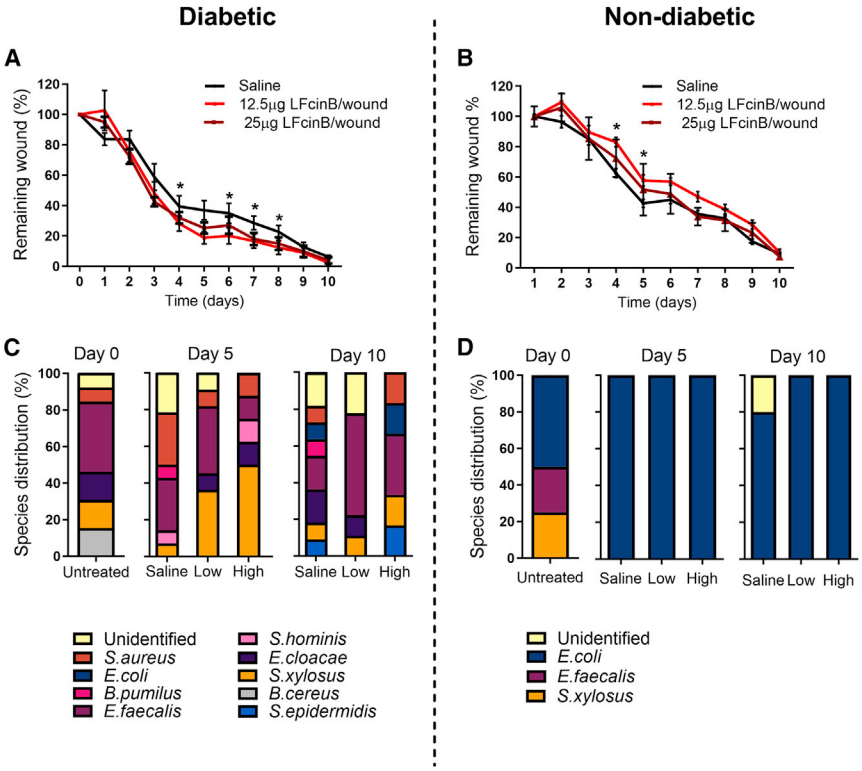

Figure 4. LFcinB enhances wound healing in diabetic but not in healthy mice

Diabetic mice (left) or healthy non-diabetic mice (right) were treated with either saline or a low (12.5 μg/wound) or high (25 μg/wound) dose of LFcinB for 10 days. Bacterial swabs were collected from the wound bed before wounding at day 0 and post-wounding at days 5 and 10, for all 3 treatment groups, followed by plating on solid media. Colonies with different morphology, size, or color were collected and identified by MALDI-TOF mass spectroscopy. (A) Diabetic mice had significantly improved wound healing at days 5 and 7–9, when treated with both low and high concentrations of LFcinB, compared with the saline treatment. (B) Healthy mice demonstrated no overall significant effects on wound closure after the LFcinB treatment. (C) A higher diversity of bacterial species was identified in the skin of diabetic mice, with *E. faecalis* being the most dominant group. (D) Low bacterial diversity was retrieved from the skin of healthy mice, with the isolated strains belonging to only 3 identifiable species, as well as an isolate of an unidentified species recovered at day 10. Treatment with LFcinB did not affect the cultured microbiome in our experimental conditions. The graph represents mean ± SD of an experiment performed with 4 mice (2 wounds/mouse) per treatment. *$p < 0.05$.

with the high dose (10.3 ± 1.9 cells/field). An increased number of M2 was likewise shown with the low dose (3.7 ± 0.56 cells/field, $p < 0.05$) compared with the high LFcinB dose (3.1 ± 0.4 cells/field). While there were clear anti-inflammatory effects of LFcinB treatment in diabetic wounds, in the non-diabetic settings the M1/M2 macrophage ratio was increased 1.6-fold (5.2 ± 0.7 versus 3.3 ± 0. 7 cells/field, $p < 0.05$) between low and high LFcinB dosage, showing a pro-inflammatory polarization of macrophages in non-diabetic wounds treated with low-dose LFcinB (Figure 5K).

Furthermore, the TNF-α mRNA expression pattern observed in the skin collected at days 0 and 10 post-wounding in both healthy and diabetic experimental groups corresponds to those already described in the literature.[4,25] At the baseline (day 0) the untreated skin from the diabetic mice had a significantly increased level of TNF-α mRNA (9.9 ± 0.4-fold) compared with non-diabetic mice (3.0 ± 1.9-fold, $p < 0.001$) (Figure S3). Treatment with LFcinB in non-diabetic mice markedly downregulated the TNF-α expression levels (0.006 ± 0.005 for low and 0.005 ± 0.001 for high concentration, $p < 0.001$) compared with saline treatment (1.0 ± 0.7). For diabetic mice, LFcinB had no effect on the mRNA levels of TNF-α (1.4 ± 1-fold, NS; 5.7 ± 5.6-fold, NS) at either low or high LFcinB dose compared with the saline treatment.

Levels of ROS in diabetic wounds were significantly increased from day 0 to day 10 independent of the treatment: saline (2.7 ± 0.6, $p < 0.01$), low LFcinB dose (2.7 ± 0.4, $p < 0.01$), and high LFcinB dose (2.4 ± 0.6, $p < 0.05$) compared with day 0 (Figure 5J). ROS production in wounds of healthy animals at day 10 was decreased by LFcinB low-dose treatment (1.7 ± 0.7, $p < 0.001$) compared with saline (4.1 ± 0.8, $p < 0.001$), but this was not the case with LFcinB high-dose treatment (3.4 ± 0.7, NS). (Figure 5L).

LFcinB enhances angiogenesis and restores collagen structure in the skin of diabetic mice

LFcinB significantly enhanced angiogenesis in wounds of diabetic mice (Figure 6A), at both the lower dose (3.1 ± 1.0, $p < 0.05$) and the higher dose (3.6 ± 0.6, $p < 0.01$), compared with saline (1.6 ± 0.3) (Figure 6E). While treatment with LFcinB increased angiogenesis in diabetic wounds, it had no effect on non-diabetic wounds (Figures 6B and 6G). The average number of new blood vessels in healthy animals was significantly decreased with the low-dose of LFcinB (1.1 ± 0.03, $p < 0.05$) compared with saline (1.8 ± 0.3), and no significant effect was shown for the higher dose (1.5 ± 0.4, NS) (Figure 6G).

The final phase of wound healing involves collagen remodeling, providing the integrity and strength of the tissue and collagen fiber-enriched scar.[26] With the Masson's trichrome stain (Figures 6C and 6D), collagen deposition and other skin structures like adipose tissue and hair follicles were visualized in the wounded skin. The collagen fibers were restored in both diabetic (3.0 ± 0.7, $p < 0.05$) and non-diabetic (3.8 ± 1.2, $p < 0.05$) animals treated with 12.5 μg/wound LFcinB compared with saline-treated diabetic animals (1.7 ± 0.3) and healthy controls (1.5 ± 0.8), while there was no effect of 25 μg/wound LFcinB on collagen restoration for either the diabetic or healthy

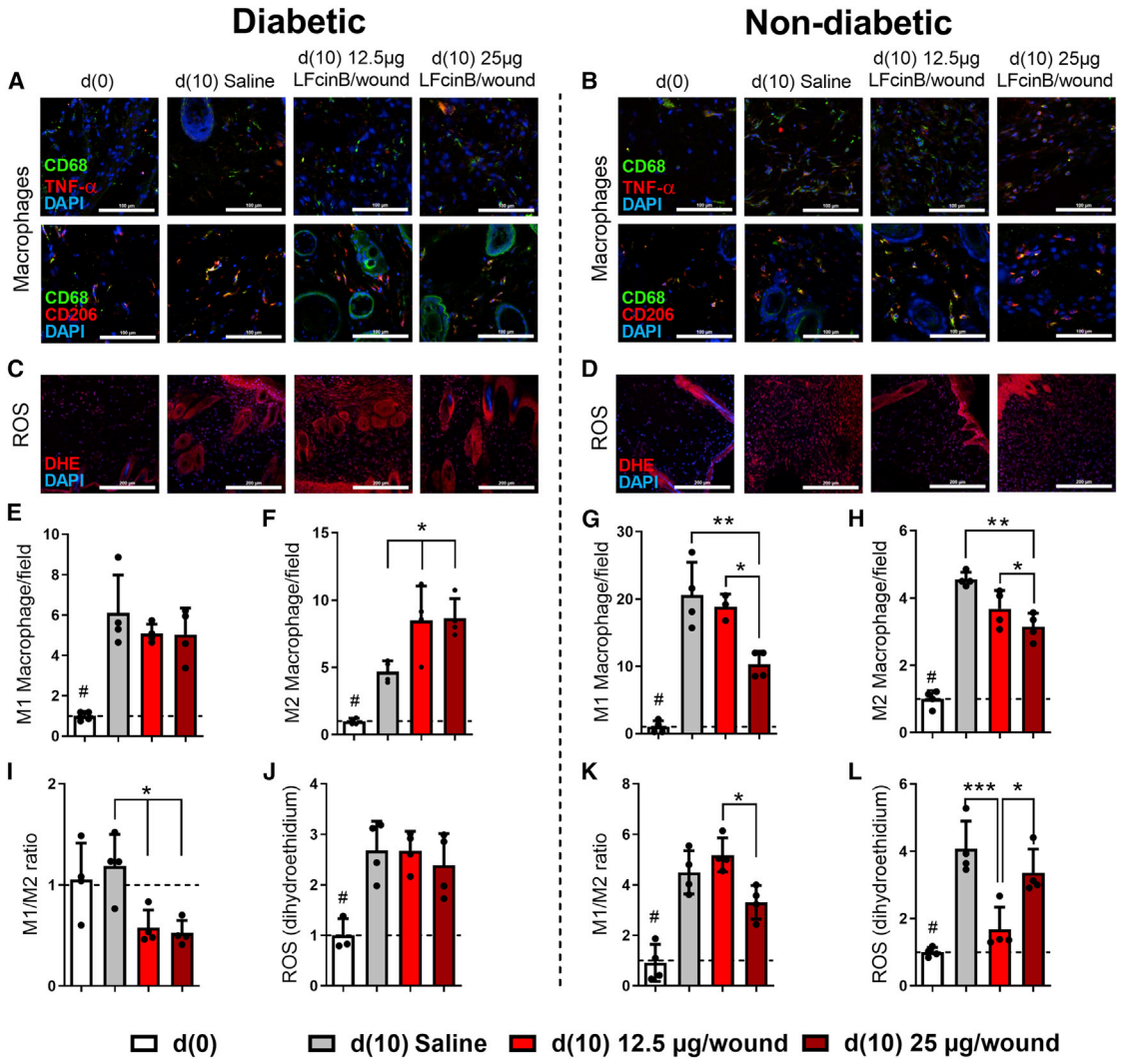

Figure 5. Immunofluorescence analysis of macrophage abundance and phenotype and production of reactive oxygen species (ROS) in diabetic and non-diabetic mouse skin treated with LFcinB

Diabetic mice (left) or healthy non-diabetic mice (right) were treated either with saline or with a low (12.5 µg/wound) or high (25 µg/wound) dose of LFcinB for 10 days. (A and B) Representative confocal microscopy images of CD68/TNF-α (M1 macrophages) and CD68/CD206 (M2 macrophages) positive stained cells in diabetic and healthy mouse skin sections. (C and D) Representative images of ROS production in murine wound skin measured by dihydroethidium (DHE) staining in diabetic or healthy animals. (E–H) The number of macrophages was quantified as the average number of CD68 positive cells co-stained with TNF-α for M1 and CD206 for M2 macrophages. (I and K) Pro-inflammatory/anti-inflammatory phenotype evaluated as M1/M2 ratio for diabetic or healthy mice. (J and L) ROS were measured as integrated density gray value after detection of the red signal of DHE staining in diabetic or healthy skin sections. Magnifications, 400× for CD68/TNF-α and CD68/CD206 and 200× for DHE. Scale bars, 100 µm for CD68/TNF-α and CD68/CD206 and 200 µm for DHE. The graph represents mean ± SD of an experiment (n = 4 animals per group), comparing the difference between the saline and treatment groups or between treatment groups (*) and the comparison of saline to baseline (#).$^{*,\#}p < 0.05$, $^{**}p < 0.01$, $^{***}p < 0.001$.

mice (1.7 ± 0.4 and 1.5 ± 0.8, respectively) (Figures 6F and 6H). Together, these findings are in concordance with the observed wound healing effect (Figure 4) and the change to an anti-inflammatory macrophage polarization in diabetic animals (Figure 5).

DISCUSSION

Current attempts to promote healing in chronic wounds are many,[27] and antimicrobial treatments yield promising results.[28] Beyond direct antimicrobial activity, antimicrobial peptides (AMPs) also induce strong anti-inflammatory response to bacterial toxins like LPS (endotoxins) for Gram-negative or lipoproteins and for Gram-positive bacterial strains.[29]

Only a few studies have investigated the role of LFcinB in wound healing, and to the best of our knowledge no study has investigated its effects on keratinocyte migration. While LFcinB robustly increased

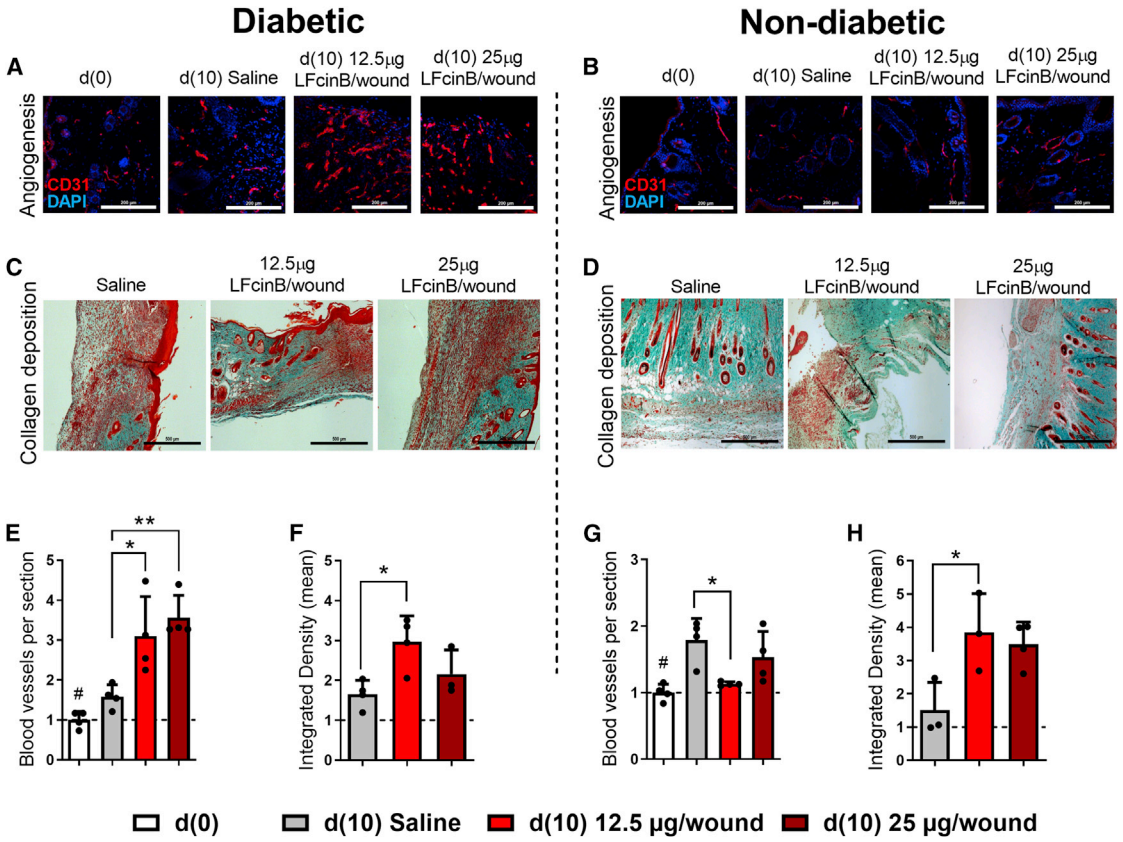

Figure 6. Topical treatment with LFcinB improves vascular network and collagen deposition in mouse wounds

Diabetic (left) and non-diabetic animals (right). (A and B) Angiogenesis was assayed as immunofluorescence of CD31-positive cells in skin sections after LFcinB treatment in diabetic and non-diabetic mice. (C and D) Representative photomicrographs of the Masson trichrome staining of (C) diabetic and (D) non-diabetic mouse skin, harvested after 10 consecutive days of treatment with saline or LFcinB at 12.5 μg/wound or 25 μg/wound. (E and G) Quantification of CD31 staining showing the mean number of newly formed blood vessels in (E) diabetic animals or (G) non-diabetic controls. (F and H) Collagen bundles were quantified and presented as the mean signal and integrated density gray values of blue channel in (F) diabetic and (H) healthy mice. Magnifications, 200× for CD31 and 100× for Masson's trichrome staining. Scale bars, 200 μm for CD31 and 500 μm for Masson's trichrome. The graphs represent mean ± SD of an experiment (n = 4 animals per group), indicating the difference between the saline and treatment groups on day 10 (*) and the saline and peptide treatments in comparison to baseline (#). *$p < 0.05$, **$p < 0.01$.

HaCaT cell migration, bLF had no effect (Figures 1A and 1B), as previously demonstrated.[30] We did not observe an effect of LFcinB on HaCaT cell proliferation (Figure S1). These data are concordant with previous observations in cancer cells,[31] and in an endothelial cell line,[32] showing that LFcinB does not affect proliferation in concentrations below 200 μg/mL. However, for proliferation conflicting data have been reported: Some studies show effects,[30,33] while others do not.[34,35] During wounding, there often is a loss of tissue, and therefore an increase of proliferation would help the close and re-form the lost tissue. A previous study observed that hLF and LFcinB had different uptake and distribution in eukaryotic cells. hLF was taken into the cell by endocytosis, whereas LFcinB was freely distributed in the cytoplasm without signs of endosomes.[8] Interestingly, the hLF was mainly found on the cell surface and some in the cytoplasm, but captured in an endosome, which could explain the difference in HaCaT migration. hLF and bLF are 69% homologous and share many conserved regions and functions.[36] It is therefore possible that the different migratory effects between bLF and LFcinB are due to the different uptake and release inside the cells. In our studies, we observed LFcinB to potently stimulate migration at a concentration of just 25 μg/mL with no associated cell toxicity.

Chronic wounds in patients with diabetes are described as stalled in a persistent inflammatory condition stamped by increment of pro-inflammatory molecules. A variety of chemokines and cytokines detected at the wound site upon injury are important chemoattractants for leukocytes, although not all appear to have critical roles during wound healing.[37]

Our findings show significant reduction in mRNA expression levels for TNF-α, IL-6, and IL-8 in HaCaT cells upon 24 h treatment with either LFcinB or bLF (Figure 1C). Previous studies indicate that EGF treatment reduces the levels of pro-inflammatory cytokines.[38–40] TNF-α, a crucial cytokine for wound healing, during the

first 24 h post-injury was found upregulated in chronic wounds[41] along with IL-8.[42] TNF-α secretion from PBMCs was found increased in the presence of LPS. Moreover, upon co-stimulation with LFcinB and LPS the TNF-α levels secreted from human primary PBMCs were found to be significantly decreased compared with LPS-only treated control (Figure 2A).

Analysis of chronic wound fluids found significantly elevated levels of pro-inflammatory cytokines IL-1, IL-6, and TNF-α.[43] Interestingly, the levels of these cytokines are restored to basal levels during the later phases of wound healing.[43,44] These pro-inflammatory cytokines are deregulated in diabetic patients.[45] Reducing the levels of these markedly expressed cytokines, like IL-6 and IL-8, is necessary for the proper healing of wounds.[46,47] Moreover, the strong reduction of TNF-α could potentially mediate the inhibition of IL-8, as TNF-α has been shown to upregulate IL-6, IL-8, and TNF-α itself.[48]

Decreased levels of MCP-1 play a role in modulating several processes involved in wound healing, such as delayed re-epithelialization, dysfunctional angiogenesis, and impaired collagen formation.[49,50] Given the importance of monocytes/macrophages for their response during early and late phases of healing under diabetic conditions, increased levels of MCP-1 have been implicated in chronic wounds by stimulating macrophage migration toward the wound site.[37,50] LFcinB has previously been reported to bind LPS[51,52] and other negatively charged molecules.[53] Here, we demonstrate that LFcinB could not diminish LPS-induced levels of MCP-1 secreted from HaCaT (Figure 1D) and PBMCs (Figure 2B). Conversely, LPS-stimulated human PBMCs released significantly higher levels of MCP-1 upon addition of LFcinB (Figure 2B).

In addition to *in vitro* experiments, we tested the effect of LFcinB treatments using an *ex vivo* model of porcine ears and *in vivo* in mice using a model of impaired wound healing, comparing the peptide effects on healthy and diabetic animals.

The porcine skin model has been considered the best model for human skin because of its similarities,[54] having similar anatomy and composition,[20] ease of transdermal drug delivery,[55–57] and immune cell responses.[58] Additionally, pig skin resembles human skin, with tightly connected skin layers, whereas rodents have loosely connected skin. Pigs have similar host defense peptides such as LF and LFcinB, but they also express peptides not found in humans.[59,60] LFcinB promoted epithelial closure in this *ex vivo* wound healing model of primary porcine keratinocytes, which was accompanied by subsequent increase in epithelial cell proliferation from day 3 to day 5 (Figure 3C). Thus, the *ex vivo* model showed an increase in proliferation, whereas the *in vitro* model did not (Figure S1). The reason behind these contradictory results is not clear, and further investigation is necessary. However, cationic peptides have previously been demonstrated to enhance key growth factors that are crucial for healing.[61]

The streptozotocin-induced diabetic mouse has some advantages with regard to chronic wound studies. These mouse wounds share fundamental similarities with wounds in diabetic patients. Diabetic mouse wounds present reduced peripheral nerve function, blood vessel numbers, granulation tissue formation, and collagen composition, making them a widely accepted *in vivo* model for diabetic wound healing.[62,63] Moreover, previous findings that murine skin heals by contraction whereas human skin heals by re-epithelialization, during which keratinocytes populate the granulation tissue to close the wound, have been revised, showing that mice heal by both contraction and re-epithelialization, making them valid models of human wound healing.[64] Upon *in vivo* topical treatments in our pre-clinical model, it was evident that LFcinB improved wound healing only under diabetic and not normoglycemic conditions. Such divergent effects of AMPs in diabetic wound healing have been observed before.[65] This was further associated with modulation of bacterial diversity, possibly toward a more commensal profile in diabetic but not healthy animals (Figures 4A and 4B). A possible explanation for these apparently contradictory effects on wound healing and bacterial diversity could be the altered immune or inflammatory response observed in diabetic mice, as AMPs often play immunomodulatory roles.

Culture-based methods are biased toward microorganisms that are best adapted to laboratory settings and are only a representative snapshot of the total diabetic foot ulcer colonizers that often also include diverse fastidious microorganisms, anaerobes, and fungal communities.[66] Nevertheless, this approach allows the interpretation of observed changes in the microbial community structure resulting from the effect of a single antimicrobial agent. Considering that the murine and human microbiomes are different in diversity and structure,[67] and that colonization depends on particular environmental factors, the results reported here represent only a fraction of the mouse skin microbiome[68] and are therefore not representative of the human skin microbiome. However, our results clearly indicate that the improved wound healing observed in the diabetic wounds is accompanied by a decrease in the complexity and composition of the bacterial species populating the wounds.

A higher diversity of bacterial strains was obtained from diabetic mice compared with non-diabetic mice (Figures 4C and 4D). Cultivated strains included species from the *Firmicutes* (*Staphylococcus* spp., *Bacillus* spp.) and from *Proteobacteria* (*Escherichia* sp., *Enterobacter* spp.) phyla, commonly present in the human skin environment. It has been reported that diabetic patients have increased bacterial diversity, in which decreased *Staphylococcus* spp. levels are observed compared with healthy controls.[69]

Treatment with LFcinB decreased strain diversity in the wounds at both concentrations (Figure 4C). Of note, *B. pumilus*, often identified in clinical isolates,[70] was only identified in diabetic and not in non-diabetic wound beds. In addition, this species completely disappeared with the LFcinB treatment. LFcinB is a known AMP active against various bacteria with MIC/minimal bactericidal concentration of 32/64 μg/mL and 16/32 μg/mL against *E. coli* and *S. aureus*, respectively, and 6/16 μg/mL against *B. subtilis*.[24] Notably, the relative abundance of *S. aureus* levels seems to decrease after treatment

with both concentrations of LFcinB (day 5), an observation that seemed to be more pronounced at day 10 for the lowest LFcinB concentration (Figure 4C). Concomitantly, LFcinB treatment led to an increase of the relative levels of commensal *S. xylosus* (day 5) and of *S. epidermidis* (day 10), which suggests that the apparent positive effect of LFcinB in the multifactorial process of diabetic wound healing may also involve a combined antimicrobial effect toward the pathogenic species of *Staphylococcus* and a stimulating effect on the commensal species. Although these remain to be experimentally verified, the hypothesis underlines that the microbiome of diabetic wounds remains poorly understood, highlighting that additional and more comprehensive studies in this unique ecosystem are required.

AMPs possess antimicrobial and anti-toxin activity as well as immunomodulatory features, which are often physiologically relevant. AMPs may also facilitate pathogen eradication by modulating cellular immune responses, such as downregulating the levels of pro-inflammatory cytokines, altering chemokine expression and ROS and reactive nitrogen species, stimulating angiogenesis, improving wound healing, and activating and/or differentiating skin immune cells.[71] In our studies, LFcinB treatment affected most of these aspects of wound healing.

Inflammatory cell infiltration, along with the proliferation of fibroblasts and endothelial cells, is a critical component of the healing process.[72] Our histological evaluations showed improved structure of granulation tissue in the dermis of diabetic mice at a higher rate than in the healthy animals. Sections of wounded tissue at day 10 post-wounding showed increased infiltration of macrophages/fibroblasts and edematous and hemorrhagic spots in saline- and LFcinB-treated healthy animals. In contrast, no edema, lower polymorphonuclear neutrophil density, and higher macrophage/fibroblast abundance were observed in diabetic animals treated with LFcinB compared with the saline diabetic group and healthy control animals (Figure S2). We have observed similar findings with significantly decreased TNF-α levels with LFcinB and LPS secreted from PBMCs and increased secretion of MCP-1 triggered by LPS stimulation, which may partially explain the reduced bacterial load and better control of wound bed inflammatory status upon LFcinB treatment.[51–53]

Wound healing deterioration by aberrant macrophage regulation is one of the crucial pathologies associated with diabetic wounds.[73] The resolution of inflammation requiring the conversion from pro- to anti-inflammatory state will thus delay the inflammatory phase if aberrant M1-to-M2 macrophage shift occurs.[74–76] Pro- and anti-inflammatory phenotypes of highly abundant macrophages, recognized with routine histological staining, were further distinguished with immunolabeling with specific antibodies. The improved diabetic wound healing we have observed in our animal model with diabetic animals was marked by a higher number of M2 over M1 macrophages (Figure 5).

High TNF-α levels were observed comparing the diabetic and healthy animals at the baseline (Figure S3). The persistent chronic inflammatory environment within chronic wounds results in high oxidative stress[77,78] and low oxygen levels.[79,80] High and sustained levels of ROS have been detected in humans and have been described as the permanent obstacle of cellular function and correct wound repair in chronic, non-healing wounds.[77,81] The full-length bLF is an antioxidant[82] and it was therefore relevant to assess the effect of LFcinB on ROS levels in diabetic as well as non-diabetic wounds. Although the downregulation of intracellular ROS levels by bLF has been documented in other studies,[83] for LFcinB decreased ROS levels were only observed with the low LFcinB dose (Figure 5); however, more studies are needed to fully investigate this.

The decreased inflammatory environment following LFcinB treatment of diabetic mouse wounds was accompanied by increased angiogenesis and increased collagen deposition reflecting improved progression through the phases of wound healing (Figure 6). Numerous studies propose insufficient angiogenesis as an underlying defect involved in the pathology of wound healing under diabetic conditions.[84–88] In the proliferative phase, angiogenesis and epithelialization are of particular importance.[89,90]

LFcinB has previously been demonstrated to inhibit growth factors, such as vascular endothelial growth factor (VEGF), *in vitro*,[27] potentially explaining the positive effect on the *ex vivo* and diabetic wound models.

The interaction with macrophages at the inflammation site restrains the production of inflammatory cytokines,[91] which further promotes establishment of the environmental niche for neovascularization.[85] Here, we report improved angiogenesis by treatment with LFcinB; however, this proposed mechanism remains to be further investigated.

A significant difference in the collagen density and organization in the healing dermis was observed between diabetic and healthy animals upon LFcinB treatment (Figure 6). Notably, the presence of thick, well-organized collagen bundles in the diabetic group treated with lower-dose LFcinB was comparable to the higher-dose and saline groups and the effect of the peptide in healthy animals. These findings illustrate that LFcinB can improve the density and deposition of collagen structure in diabetic wound healing through reinforcing the function of skin cells.

The exact mechanism behind the observed improvement of wound healing mediated by LFcinB as observed in *in vitro*, *ex vivo*, and *in vivo* models could in part be explained by its combined ability to enhance migration and cell proliferation, to modulate the bacterial composition in the wound, and by its ability to diminish LPS- or wound-induced pro-inflammatory cytokine expression as seen for TNF-α both *in vitro* and *in vivo*. Although we propose a possible association between the microbial-modulating and immunomodulatory properties of LFcinB, additional studies are needed in order to obtain further knowledge on the molecular mechanisms underlying these properties.

MATERIALS AND METHODS

Peptides

bLF was purchased from Sigma (146897-68-9, USA), and LFcinB was kindly received from Dr. Ron Marschke from the Center for Food Technology (Australia). All peptides were dissolved in saline (sterile H_2O with 0.85% NaCl).

Migration and proliferation of HaCaT cells

Immortalized keratinocytes (HaCaT cells)[92] were kindly donated from Bispebjerg Hospital. The HaCaT cell line was maintained in DMEM with 25 mM glucose, containing GlutaMAX (31966-021, Thermo Fisher, USA), 10% FBS (10270, Gibco, USA), and 100 units/mL penicillin and streptomycin (P0781, Sigma-Aldrich, USA). The cells were cultured in T75 flasks, and sub-cultured twice weekly. The migration assay was performed exactly as described previously.[93] Briefly, 7.5×10^4 cells were transferred to a 48-well plate and allowed to adhere overnight at 37°C in a 5% CO_2 incubator. The cells were mitomycin C (3258, Tocris, UK) (10 μg/mL) treated to inhibit proliferation for 2 h as previously demonstrated.[94] Scratches were made with a 200 μL pipette tip in PBS. LFcinB and EGF (Sigma-Aldrich) were diluted in DMEM to final concentrations of 25 μg/mL and 100 ng/mL, respectively. Migration of the cells was monitored with an automated optical camera (oCelloScope, BioSense, Denmark), at 37°C and 5% CO_2. The oCelloScope was set to follow wells for 48 h and acquire images every 12th hour. The migratory effects were calculated as a percentage of the gap closure. Proliferation was likewise performed in a 48-well plate with 1×10^4 cells/well (10% confluence). After adhesion, the same treatments were administered, the plate was incubated in the oCelloScope, and cell growth was monitored. Proliferative effects were calculated as a percentage of increased amount of HaCaT cells compared to the initial number of cells.

Quantitative RT-PCR for detection of gene expression

HaCaT cells were harvested with TRI Reagent (Sigma-Aldrich), and RNA was isolated, followed by clean-up (RNeasy Plus Mini Kit, 74104, QIAGEN, USA) and cDNA synthesis (High-Capacity cDNA Reverse Transcription Kit, 4368814, Applied Biosystems, USA) as previously described.[95] Quantitative PCR (qPCR) was performed with the QuantiTect SYBR PCR Kit (204141, QIAGEN, USA) according to the protocol of the manufacturer with a Stratagene MX3005P (Agilent). The data were normalized to the reference gene RPLP0, a ribosomal gene shown to be stable in most tissues.[96] Relative gene expression was obtained according to the $\Delta\Delta C_T$ method[97]. Primer oligonucleotides have been described previously.[95]

Isolation of PBMCs and enzyme-linked immunosorbent assay (ELISA)

PBMCs were isolated from healthy donors with Ficoll-Paque PLUS (GE Healthcare, USA). After isolation, 5×10^5 cells were transferred to a 48-well plate and kept in Roswell Park Memorial Institute (RPMI)-1640 medium containing 10% FBS and 100 units/mL penicillin and streptomycin. PBMCs were treated with LFcinB at 25 μg/mL with or without LPS stimulation (from *Pseudomonas aeruginosa*, PA01) at 10, 50, or 100 ng/mL for 24 h. The media supernatant was collected after centrifugation for 3 min at 300 × *g*. The levels of TNF-α (88-7346-76) and MCP-1 (88-7399-76) were measured with an ELISA according to the protocol provided by the manufacturer (Invitrogen, USA). The secreted levels of TNF-α and MCP-1 were quantified on a spectrophotometer at 570 nm, and the background (450 nm) was subtracted. The data were normalized to cells treated with media only.

Ex vivo porcine skin wound healing model

Porcine ears, donated by the Roskilde slaughterhouse (Denmark), were collected from freshly slaughtered pigs. The ears were immediately stored on ice and thoroughly washed before use. Wounding of the skin was made as previously described.[98] Briefly, a 4 mm punch biopsy tool, a tweezer, and a scalpel were used for wounding. The wounded skin biopsies were cut to 1 cm^2 pieces, washed in 70% ethanol as previously described,[99] and transferred to sterile gauze in 12-well plates. The samples were stored in 1 mL of DMEM medium, containing 10% FBS and 100 units/mL penicillin and streptomycin, and treated with LFcinB at 25 μg/mL for 5 days post-wounding. For controls, regular media or free aa in the same mole ratio as LFcinB were used. The skin biopsies were washed twice daily in PBS before new treatments were added.

In vivo wound healing on diabetic and non-diabetic mice

Male C57BL/6 mice (25–30 g) (Charles River Corporation, Spain) were housed under a 12 h day/night cycle with water and commercial pellet food *ad libitum*. The experiment was approved by the Institutional and Governmental Research Ethical Board and was in accordance with European Community law for Experimental Animal Studies (86/609/CEE and 2007/526/CE).

Diabetic and healthy non-diabetic mice were used, where diabetes was induced 6 weeks prior to the wounding with 50 mg/kg streptozotocin (Sigma-Aldrich, USA) injected intraperitoneally for 5 consecutive days as previously described.[74] Mice with glucose levels >250 mg/dL were considered diabetic.[100] Three days pre-wounding, mice were separated into individual cages. Subcutaneous analgesics were given (0.1 mg/kg buprenorphine) before wounding and every 6–8 h up to 48 h after wounding. The mice were anesthetized with 2.5% isoflurane combined with oxygen (0.5 L/min). Dorsal hair was removed, skin was sterilized with Betadine, and two full-thickness wounds were made with a 6 mm punch biopsy tool. The mice were separated into three treatment groups: low (12.5 μg/wound) and high (25 μg/wound) LFcinB doses and saline. The doses were chosen according to the MIC of LFcinB and previous wound healing studies with cationic AMPs.[24,101] The wounds were treated topically over 10 consecutive days; twice the first 2 days and then once daily. Wound size was monitored daily and is given as percentage of closure compared to day 0. At day 10 mice were sacrificed, and skin samples were harvested for analysis.

Identification of bacterial strains in murine wounds

The recovery of bacteria from skin/wounds of animals was performed with swabs (Sarstedt) at day 0 (intact skin, before the mice were

shaved) and at days 5 and 10 post-wounding, before treatments. To maximize bacterial recovery the swabs were incubated in 1 mL of brain heart infusion broth (Becton Dickinson) with gentle agitation (120 rpm) for 3 h at 37°C. From the inoculates, 100 μL was plated on nonselective lysogeny broth (LB), chocolate agar (BD, blood agar No. 2 Base) for fastidious bacteria and on mannitol salt agar (MSA) plates for selective recovery of *Staphylococcus* spp. Colonies of different morphology (size, color, or texture) were isolated, the purity of cultures was examined, and they were stored in 15% glycerol at −80°C. Identification of bacterial species was performed by MALDI-TOF mass spectrometry (Bruker) analysis with a single colony, no older than 24 h, overlaid with Galaxy HCCA matrix (Bruker). Samples with a value of 1.70 or above were accepted.[102] Unidentified samples were re-run overlaid with a combination of 70% formic acid and Galaxy HCCA matrix to break the membrane and increase ionization.

Immunohistochemistry and histology of porcine and murine skin

Porcine skin was fixated in 4% paraformaldehyde (PFA) for histological analysis at days 0, 1, 3, and 5, paraffin embedded, and cut in 3 μm sections. Sections were stained for re-epithelialization and the number of proliferating cells with Ki67 antibody (1:800, Abcam, UK). Re-epithelialization was calculated as the percentage of epithelium covering the wound bed, whereas proliferation was calculated as the number of Ki67-positive cells per area of the epithelial layer.

The murine skin sections were preserved in cryoprotectant and fixed in buffered formalin and were cut in 10 μm (immunofluorescence)/5 μm (histology) sections. Immunohistochemical analysis was done as previously described[103] to estimate the polarization direction of the macrophages and to measure the rate of angiogenesis following the wounding. Rabbit polyclonal anti-CD68 (ab955, Abcam, UK), rabbit polyclonal anti-TNF-α (PA5-19810, Thermo Scientific, USA), rat monoclonal anti-CD206 (MR5D3) (sc-58987, Santa Cruz, USA), and rat monoclonal anti-CD31 (PECAM-1) (CBL1337, Merck Millipore, Germany) antibodies were diluted 1:100 in 2% BSA and 1% goat serum (Novex, Life Technologies, USA) in PBS. Anti-rat (conjugated to Alexa Fluor 568, Invitrogen) and anti-rabbit (Alexa Fluor 468 conjugated, Invitrogen) antibodies were diluted 1:500 in 5% BSA and 5% normal goat serum in PBS, with 0.1 volume % Triton X-100 (pH 7.4). The skin sections were fixed in ice-cold acetone for 10 min and blocked with 5% BSA for 30 min. For the primary antibody, the samples were incubated at 4°C overnight, washed in PBS, and incubated with secondary antibody and with nuclear counterstain (DAPI) (Sigma-Aldrich). Positive staining was indicated as intense red (TNF-α, CD31, CD206) or bright green (CD68) positive colored cells or vessel branches. Fluorescent images were obtained with a confocal microscope (Zeiss LSM 510 Meta), using 200× and 400× magnifications. The number of cells (n = 3 selections/6 pictures/sample) or vessels (n = 5 images/sample) expressing fluorescent signal was quantified as average number per field with Fiji software and normalized to average number of cells/vessels in biopsies at the baseline as previously reported.[74]

Hematoxylin and eosin (H&E) (Merck Millipore, Germany) and a Masson-Goldner trichrome staining kit (Carl Roth, Germany) were used for staining of murine skin as previously described[104] and were performed using 5 μm paraffin sections, according to the instructions of the manufacturer. The sections were imaged with a transmission microscope (Karl Zeiss Axio Observer Z1) at 100× and 200× magnification. Collagen density was measured as the intensity of the blue color channel, which represents the collagen, using color deconvolution in Fiji software and comparing the collagen intensity under the wound area to normal dermis at 100× magnification, as previously described[105].

Dihydroethidium assay for ROS detection

Cryopreserved skin sections (30 μm) were incubated with 10 μM dihydroethidium (DHE) (Invitrogen, USA) in a humidified dark chamber at 37°C for 30 min, followed by fixation with 4% buffered PFA for 5 min at room temperature and counterstaining with DAPI. Fluorescent images were acquired with a confocal microscope (Zeiss LSM 510 Meta) using 200× magnification (6 pictures/3 random square fields per picture for each sample). Densitometry analysis was done with Fiji software, and the DHE signal was presented as the integrated density gray mean values. Data were normalized to average integrated density values in biopsies at the baseline.

Data analysis and statistics

Statistical analyses of difference between the groups were performed with one-way ANOVA with Tukey's post hoc test or two-way ANOVA using Tukey's or Sidak's multiple comparisons tests, as appropriate. GraphPad Prism 8 was used to evaluate statistical significance. The results are expressed as means ± SD, and $p < 0.05$ was considered statistically significant.

SUPPLEMENTAL INFORMATION

Supplemental Information can be found online at https://doi.org/10.1016/j.omtm.2021.02.008.

ACKNOWLEDGMENTS

The authors would like to thank Johnny Møller for his help with this manuscript and Martin Schou Pedersen and Jesper Iversen for making it possible to work with the MALDI-TOF mass spectrometry instrument at Hvidovre Hospital, Denmark. Sónia G. Pereira (Polytechnic of Leiria, Portugal) is also acknowledged for valuable collaboration and enlightening discussions on microbial ecology. Figures were created with BioRender (Biorender.com). The *in vitro* and *ex vivo* work were funded by the Danish Council for Independent Research, Technology and Production (grant 4005-00029). Travel grants to work in Portugal were funded by Lundbeck R275-2017-2793 and Erasmus+ F2: 2015-5577. Funding for *in vivo* work was funded by FEDER-COMPETE-2020-UID/NEU/04539/2013, POCI-01-0145-FEDER-007440, UIDB/04539/2020, Healthy Aging 2020-CENTRO-01-0145-FEDER-000012-N2323, DL57/2016/CP1448/CT0024, NIGMS P20GM109096, 5P30-AG028718, and EFSD European Research Programme in Microvascular Complications/Novartis Pharma AG. Microbial sampling and isolation procedures from animals were carried out with support from the Infarmed grant FIS-FIS-2015-01_DIA_20150630-144.

AUTHOR CONTRIBUTIONS

H.J., M.V.M., and M.P. were responsible for study concept and design. M.V.M. and M.P. were responsible for initial data collection and analysis. M.V.M. and M.P. wrote the manuscript. M.V.M. and K.Q. carried out the *ex vivo* model with the guidance of S.S.P. M.V.M., M.P., and E.C.L. did the animal studies. M.V.M. and S.A. carried out the microbiological procedures for bacterial isolation. M.V.M., M.P., L.T.D., N.E., E.C., and H.J. analyzed and interpreted the data. All authors reviewed and approved the final manuscript. H.J. is the guarantor of this work and, as such, had full access to all data reported in the study and takes responsibility for the integrity of the data and the accuracy of the data analysis.

DECLARATION OF INTERESTS

The authors declare no competing interests.

REFERENCES

1. Tuttolomondo, A., Maida, C., and Pinto, A. (2015). Diabetic foot syndrome as a possible cardiovascular marker in diabetic patients. J. Diabetes Res. *2015*, 268390.
2. Merza, Z., and Tesfaye, S. (2003). The risk factors for diabetic foot ulceration. Foot *13*, 125–129.
3. Brem, H., and Tomic-Canic, M. (2007). Cellular and molecular basis of wound healing in diabetes. J. Clin. Invest. *117*, 1219–1222.
4. Graves, D.T., and Kayal, R.A. (2008). Diabetic complications and dysregulated innate immunity. Front. Biosci. *13*, 1227–1239.
5. Baltzis, D., Eleftheriadou, I., and Veves, A. (2014). Pathogenesis and treatment of impaired wound healing in diabetes mellitus: new insights. Adv. Ther. *31*, 817–836.
6. Nguyen, K.T., Seth, A.K., Hong, S.J., Geringer, M.R., Xie, P., Leung, K.P., Mustoe, T.A., and Galiano, R.D. (2013). Deficient cytokine expression and neutrophil oxidative burst contribute to impaired cutaneous wound healing in diabetic, biofilm-containing chronic wounds. Wound Repair Regen *21*, 833–841.
7. Murata, M., Wakabayashi, H., Yamauchi, K., and Abe, F. (2013). Identification of milk proteins enhancing the antimicrobial activity of lactoferrin and lactoferricin. J. Dairy Sci. *96*, 4891–4898.
8. Andersen, J.H., Jenssen, H., Sandvik, K., and Gutteberg, T.J. (2004). Anti-HSV activity of lactoferrin and lactoferricin is dependent on the presence of heparan sulphate at the cell surface. J. Med. Virol. *74*, 262–271.
9. Bellamy, W., Wakabayashi, H., Takase, M., Kawase, K., Shimamura, S., and Tomita, M. (1993). Killing of Candida albicans by lactoferricin B, a potent antimicrobial peptide derived from the N-terminal region of bovine lactoferrin. Med. Microbiol. Immunol. (Berl.) *182*, 97–105.
10. Furlong, S.J., Mader, J.S., and Hoskin, D.W. (2010). Bovine lactoferricin induces caspase-independent apoptosis in human B-lymphoma cells and extends the survival of immune-deficient mice bearing B-lymphoma xenografts. Exp. Mol. Pathol. *88*, 371–375.
11. Tang, L., Wu, J.J., Ma, Q., Cui, T., Andreopoulos, F.M., Gil, J., Valdes, J., Davis, S.C., and Li, J. (2010). Human lactoferrin stimulates skin keratinocyte function and wound re-epithelialization. Br. J. Dermatol *163*, 38–47.
12. Actor, J.K., Hwang, S.-A., and Kruzel, M.L. (2009). Lactoferrin as a natural immune modulator. Curr. Pharm. Des. *15*, 1956–1973.
13. Engelmayer, J., Blezinger, P., and Varadhachary, A. (2008). Talactoferrin stimulates wound healing with modulation of inflammation. J. Surg. Res. *149*, 278–286.
14. Bellamy, W., Takase, M., Yamauchi, K., Wakabayashi, H., Kawase, K., and Tomita, M. (1992). Identification of the bactericidal domain of lactoferrin. Biochim. Biophys. Acta *1121*, 130–136.
15. Jenssen, H. (2005). Anti herpes simplex virus activity of lactoferrin/lactoferricin – an example of antiviral activity of antimicrobial protein/peptide. Cell. Mol. Life Sci. *62*, 3002–3013.
16. Yamauchi, K., Tomita, M., Giehl, T.J., and Ellison, R.T., 3rd (1993). Antibacterial activity of lactoferrin and a pepsin-derived lactoferrin peptide fragment. Infect. Immun. *61*, 719–728.
17. Chapple, D.S., Mason, D.J., Joannou, C.L., Odell, E.W., Gant, V., and Evans, R.W. (1998). Structure-function relationship of antibacterial synthetic peptides homologous to a helical surface region on human lactoferrin against Escherichia coli serotype O111. Infect. Immun. *66*, 2434–2440.
18. Bodnar, R.J. (2013). Epidermal Growth Factor and Epidermal Growth Factor Receptor: The Yin and Yang in the Treatment of Cutaneous Wounds and Cancer. Adv. Wound Care (New Rochelle) *2*, 24–29.
19. Pier, G.B. (2007). Pseudomonas aeruginosa lipopolysaccharide: a major virulence factor, initiator of inflammation and target for effective immunity. Int. J. Med. Microbiol. *297*, 277–295.
20. Godin, B., and Touitou, E. (2007). Transdermal skin delivery: predictions for humans from in vivo, ex vivo and animal models. Adv. Drug Deliv. Rev. *59*, 1152–1161.
21. Mair, K.H., Sedlak, C., Käser, T., Pasternak, A., Levast, B., Gerner, W., Saalmüller, A., Summerfield, A., Gerdts, V., Wilson, H.L., et al. (2014). The Porcine Innate Immune System: An Update (Elsevier).
22. Seaton, M., Hocking, A., and Gibran, N.S. (2015). Porcine models of cutaneous wound healing. ILAR J. *56*, 127–138.
23. Corsetti, G., D'Antona, G., Dioguardi, F.S., and Rezzani, R. (2010). Topical application of dressing with amino acids improves cutaneous wound healing in aged rats. Acta Histochem. *112*, 497–507.
24. Liu, Y., Han, F., Xie, Y., and Wang, Y. (2011). Comparative antimicrobial activity and mechanism of action of bovine lactoferricin-derived synthetic peptides. Biometals *24*, 1069–1078.
25. Hotamisligil, G., Shargill, N., and Spiegelman, B. (1993). Adipose expression of tumor necrosis factor-alpha: direct role in obesity-linked insulin resistance. Science *259*, 87–91.
26. Volk, S.W., Wang, Y., Mauldin, E.A., Liechty, K.W., and Adams, S.L. (2011). Diminished type III collagen promotes myofibroblast differentiation and increases scar deposition in cutaneous wound healing. Cells Tissues Organs *194*, 25–37.
27. Chin, J.S., Madden, L., Chew, S.Y., and Becker, D.L. (2019). Drug therapies and delivery mechanisms to treat perturbed skin wound healing. Adv. Drug Deliv. Rev. *149-150*, 2–18.
28. Chen, L., and Harrison, S.D. (2007). Cell-penetrating peptides in drug development: enabling intracellular targets. Biochem. Soc. Trans. *35*, 821–825.
29. Brandenburg, K., Heinbockel, L., Correa, W., and Lohner, K. (2016). Peptides with dual mode of action: Killing bacteria and preventing endotoxin-induced sepsis. Biochim. Biophys. Acta *1858*, 971–979.
30. Duarte, D.C., Nicolau, A., Teixeira, J.A., and Rodrigues, L.R. (2011). The effect of bovine milk lactoferrin on human breast cancer cell lines. J. Dairy Sci. *94*, 66–76.
31. Wang, S., Tu, J., Zhou, C., Li, J., Huang, L., Tao, L., and Zhao, L. (2015). The effect of Lfcin-B on non-small cell lung cancer H460 cells is mediated by inhibiting VEGF expression and inducing apoptosis. Arch. Pharm. Res. *38*, 261–271.
32. Mader, J.S., Smyth, D., Marshall, J., and Hoskin, D.W. (2006). Bovine lactoferricin inhibits basic fibroblast growth factor- and vascular endothelial growth factor165-induced angiogenesis by competing for heparin-like binding sites on endothelial cells. Am. J. Pathol. *169*, 1753–1766.
33. Shimamura, M., Yamamoto, Y., Ashino, H., Oikawa, T., Hazato, T., Tsuda, H., and Iigo, M. (2004). Bovine lactoferrin inhibits tumor-induced angiogenesis. Int. J. Cancer *111*, 111–116.
34. Blais, A., Fan, C., Voisin, T., Aattouri, N., Dubarry, M., Blachier, F., and Tomé, D. (2014). Effects of lactoferrin on intestinal epithelial cell growth and differentiation: an in vivo and in vitro study. Biometals *27*, 857–874.
35. Buccigrossi, V., de Marco, G., Bruzzese, E., Ombrato, L., Bracale, I., Polito, G., and Guarino, A. (2007). Lactoferrin induces concentration-dependent functional modulation of intestinal proliferation and differentiation. Pediatr. Res. *61*, 410–414.
36. Jenssen, H., and Hancock, R.E.W. (2009). Antimicrobial properties of lactoferrin. Biochimie *91*, 19–29.

37. Engelhardt, E., Toksoy, A., Goebeler, M., Debus, S., Bröcker, E.B., and Gillitzer, R. (1998). Chemokines IL-8, GROalpha, MCP-1, IP-10, and Mig are sequentially and differentially expressed during phase-specific infiltration of leukocyte subsets in human wound healing. Am. J. Pathol. *153*, 1849–1860.

38. Choi, S.Y., Lee, Y.J., Kim, J.M., Kang, H.J., Cho, S.H., and Chang, S.E. (2018). Epidermal Growth Factor Relieves Inflammatory Signals in Staphylococcus aureus-Treated Human Epidermal Keratinocytes and Atopic Dermatitis-Like Skin Lesions in Nc/Nga Mice. Biomed Res. Int *2018*, 9439182.

39. Kim, Y.J., Choi, M.J., Bak, D.H., Lee, B.C., Ko, E.J., Ahn, G.R., Ahn, S.W., Kim, M.J., Na, J., and Kim, B.J. (2018). Topical administration of EGF suppresses immune response and protects skin barrier in DNCB-induced atopic dermatitis in NC/Nga mice. Sci. Rep. *8*, 11895.

40. Wang, L., Huang, Z., Huang, W., Chen, X., Shan, P., Zhong, P., Khan, Z., Wang, J., Fang, Q., Liang, G., and Wang, Y. (2017). Inhibition of epidermal growth factor receptor attenuates atherosclerosis via decreasing inflammation and oxidative stress. Sci. Rep. *8*, 45917.

41. Ashcroft, G.S., Jeong, M.-J.J., Ashworth, J.J., Hardman, M., Jin, W., Moutsopoulos, N., Wild, T., McCartney-Francis, N., Sim, D., McGrady, G., et al. (2012). Tumor necrosis factor-alpha (TNF-α) is a therapeutic target for impaired cutaneous wound healing. Wound Repair Regen. *20*, 38–49.

42. Satish, L. (2015). Chemokines as Therapeutic Targets to Improve Healing Efficiency of Chronic Wounds. Adv. Wound Care (New Rochelle) *4*, 651–659.

43. Harris, I.R., Yee, K.C., Walters, C.E., Cunliffe, W.J., Kearney, J.N., Wood, E.J., and Ingham, E. (1995). Cytokine and protease levels in healing and non-healing chronic venous leg ulcers. Exp. Dermatol. *4*, 342–349.

44. Ritsu, M., Kawakami, K., Kanno, E., Tanno, H., Ishii, K., Imai, Y., Maruyama, R., and Tachi, M. (2017). Critical role of tumor necrosis factor-α in the early process of wound healing in skin. J. Dermatol. Dermatol. Surg. *21*, 14–19.

45. King, G.L. (2008). The role of inflammatory cytokines in diabetes and its complications. J. Periodontol. *79* (8, Suppl), 1527–1534.

46. Lin, Z.-Q., Kondo, T., Ishida, Y., Takayasu, T., and Mukaida, N. (2003). Essential involvement of IL-6 in the skin wound-healing process as evidenced by delayed wound healing in IL-6-deficient mice. J. Leukoc. Biol. *73*, 713–721.

47. Jiang, W.G., Sanders, A.J., Ruge, F., and Harding, K.G. (2012). Influence of interleukin-8 (IL-8) and IL-8 receptors on the migration of human keratinocytes, the role of PLC-γ and potential clinical implications. Exp. Ther. Med *8*, 231–236.

48. Sedger, L.M., and McDermott, M.F. (2014). TNF and TNF-receptors: From mediators of cell death and inflammation to therapeutic giants—past, present and future. Cytokine Growth Factor Rev. *25*, 453–472.

49. Low, Q., Drugea, I., Duffner, L., Quinn, D., Cook, D., Rollins, B., Kovacs, E., and DePietro, L. (2001). Wound healing in MIP-1a$^{-/-}$ and MCP-1$^{-/-}$ Mice. Am. J. Pathol. *159*, 457–463.

50. Wood, S., Jayaraman, V., Huelsmann, E.J., Bonish, B., Burgad, D., Sivaramakrishnan, G., Qin, S., DiPietro, L.A., Zloza, A., Zhang, C., and Shafikhani, S.H. (2014). Pro-inflammatory chemokine CCL2 (MCP-1) promotes healing in diabetic wounds by restoring the macrophage response. PLoS ONE *9*, e91574.

51. Samuelsen, Ø., Haukland, H.H., Ulvatne, H., and Vorland, L.H. (2004). Anti-complement effects of lactoferrin-derived peptides. FEMS Immunol. Med. Microbiol. *41*, 141–148.

52. Vorland, L.H., Ulvatne, H., Rekdal, O., and Svendsen, J.S. (1999). Initial binding sites of antimicrobial peptides in Staphylococcus aureus and Escherichia coli. Scand. J. Infect. Dis. *31*, 467–473.

53. Britigan, B.E., Lewis, T.S., Waldschmidt, M., McCormick, M.L., and Krieg, A.M. (2001). Lactoferrin binds CpG-containing oligonucleotides and inhibits their immunostimulatory effects on human B cells. J. Immunol. *167*, 2921–2928.

54. Sullivan, T.P., Eaglstein, W.H., Davis, S.C., and Mertz, P. (2001). The pig as a model for human wound healing. Wound Repair Regen. *9*, 66–76.

55. Summerfield, A., Meurens, F., and Ricklin, M.E. (2015). The immunology of the porcine skin and its value as a model for human skin. Mol. Immunol. *66*, 14–21.

56. Kong, R., and Bhargava, R. (2011). Characterization of porcine skin as a model for human skin studies using infrared spectroscopic imaging. Analyst (Lond.) *136*, 2359–2366.

57. Tfaili, S., Gobinet, C., Josse, G., Angiboust, J.F., Manfait, M., and Piot, O. (2012). Confocal Raman microspectroscopy for skin characterization: a comparative study between human skin and pig skin. Analyst (Lond.) *137*, 3673–3682.

58. Meurens, F., Summerfield, A., Nauwynck, H., Saif, L., and Gerdts, V. (2012). The pig: a model for human infectious diseases. Trends Microbiol. *20*, 50–57.

59. Sang, Y., and Blecha, F. (2009). Porcine host defense peptides: expanding repertoire and functions. Dev. Comp. Immunol. *33*, 334–343.

60. Hajji, M., Jellouli, K., Hmidet, N., Balti, R., Sellami-Kamoun, A., and Nasri, M. (2010). A highly thermostable antimicrobial peptide from Aspergillus clavatus ES1: biochemical and molecular characterization. J. Ind. Microbiol. Biotechnol. *37*, 805–813.

61. Marin-Luevano, P., Trujillo, V., Rodriguez-Carlos, A., González-Curiel, I., Enciso-Moreno, J.A., Hancock, R.E.W., and Rivas-Santiago, B. (2018). Induction by innate defence regulator peptide 1018 of pro-angiogenic molecules and endothelial cell migration in a high glucose environment. Peptides *101*, 135–144.

62. Mestas, J., and Hughes, C.C.W. (2004). Of mice and not men: differences between mouse and human immunology. J. Immunol. *172*, 2731–2738.

63. Nunan, R., Harding, K.G., and Martin, P. (2014). Clinical challenges of chronic wounds: searching for an optimal animal model to recapitulate their complexity. Dis. Model. Mech. *7*, 1205–1213.

64. Chen, L., Mirza, R., Kwon, Y., DiPietro, L.A., and Koh, T.J. (2015). The murine excisional wound model: Contraction revisited. Wound Repair Regen. *23*, 874–877.

65. Steinstraesser, L., Hirsch, T., Schulte, M., Kueckelhaus, M., Jacobsen, F., Mersch, E.A., Stricker, I., Afacan, N., Jenssen, H., Hancock, R.E.W., and Kindrachuk, J. (2012). Innate Defense Regulator Peptide 1018 in Wound Healing and Wound Infection. PLoS One *7*, e39373.

66. Kalan, L., Loesche, M., Hodkinson, B.P., Heilmann, K., Ruthel, G., Gardner, S.E., and Grice, E.A. (2016). Redefining the chronic-wound microbiome: Fungal communities are prevalent, dynamic, and associated with delayed healing. MBio *7*, e01058, 16.

67. Lagkouvardos, I., Pukall, R., Abt, B., Foesel, B.U., Meier-Kolthoff, J.P., Kumar, N., Bresciani, A., Martínez, I., Just, S., Ziegler, C., et al. (2016). The Mouse Intestinal Bacterial Collection (miBC) provides host-specific insight into cultured diversity and functional potential of the gut microbiota. Nat. Microbiol. *1*, 16131, 15.

68. Rosshart, S.P., Herz, J., Vassallo, B.G., Hunter, A., Wall, M.K., Badger, J.H., McCulloch, J.A., Anastasakis, D.G., Sarshad, A.A., Leonardi, I., et al. (2019). Laboratory mice born to wild mice have natural microbiota and model human immune responses. Science *365*, eaaw4361.

69. Redel, H., Gao, Z., Li, H., Alekseyenko, A.V., Zhou, Y., Perez-Perez, G.I., Weinstock, G., Sodergren, E., and Blaser, M.J. (2013). Quantitation and composition of cutaneous microbiota in diabetic and nondiabetic men. J. Infect. Dis. *207*, 1105–1114.

70. Celandroni, F., Salvetti, S., Gueye, S.A., Mazzantini, D., Lupetti, A., Senesi, S., and Ghelardi, E. (2016). Identification and Pathogenic Potential of Clinical Bacillus and Paenibacillus Isolates. PLoS ONE *11*, e0152831.

71. Hilchie, A.L., Wuerth, K., and Hancock, R.E.W. (2013). Immune modulation by multifaceted cationic host defense (antimicrobial) peptides. Nat. Chem. Biol. *9*, 761–768.

72. Goh, E.T., Kirby, G., Rajadas, J., Liang, X.J., and Tan, A. (2016). Accelerated Wound Healing Using Nanoparticles. In Nanoscience in Dermatology, M.R. Hamblin, P. Avci, and T.W. Prow, eds. (Elsevier), pp. 287–306.

73. Wicks, K., Torbica, T., and Mace, K.A. (2014). Myeloid cell dysfunction and the pathogenesis of the diabetic chronic wound. Semin. Immunol. *26*, 341–353.

74. Leal, E.C., Carvalho, E., Tellechea, A., Kafanas, A., Tecilazich, F., Kearney, C., Veves, A., Kuchibhotla, S., Auster, M.E., Kokkotou, E., et al. (2015). Substance P Promotes Wound Healing in Diabetes by Modulating Inflammation and Macrophage Phenotype. Am. J. Pathol *185*, 1638–1648.

75. Landén, N.X., Li, D., and Ståhle, M. (2016). Transition from inflammation to proliferation: a critical step during wound healing. Cell. Mol. Life Sci. *73*, 3861–3885.

76. Larouche, J., Sheoran, S., Maruyama, K., and Martino, M.M. (2018). Immune regulation of skin wound healing: Mechanisms and novel therapeutic targets. Adv. Wound Care (New Rochelle) *7*, 209–231.

77. Schäfer, M., and Werner, S. (2008). Oxidative stress in normal and impaired wound repair. Pharmacol. Res. *58*, 165–171.

78. Abd-El-Aleem, S.A., Ferguson, M.W.J., Appleton, I., Kairsingh, S., Jude, E.B., Jones, K., McCollum, C.N., and Ireland, G.W. (2000). Expression of nitric oxide synthase isoforms and arginase in normal human skin and chronic venous leg ulcers. J. Pathol. *191*, 434–442.

79. Babior, B.M. (1978). Oxygen-Dependent Microbial Killing by Phagocytes. N. Engl. J. Med *298*, 659–668.

80. Segal, A.W. (2008). How superoxide production by neutrophil leukocytes kills microbes. In Innate Immunity to Pulmonary Infection, D.J. Chadwick and J. Goode, eds. (Novartis Foundation), pp. 92–100.

81. Zhao, R., Liang, H., Clarke, E., Jackson, C., and Xue, M. (2016). Inflammation in chronic wounds. Int. J. Mol. Sci. *17*, 2085.

82. Park, S.Y., Jeong, A.J., Kim, G.Y., Jo, A., Lee, J.E., Leem, S.H., Yoon, J.H., Ye, S.K., and Chung, J.W. (2017). Lactoferrin protects human mesenchymal stem cells from oxidative stress-induced senescence and apoptosis. J. Microbiol. Biotechnol. *27*, 1877–1884.

83. El-Desouky, M.A., Osman, S., Shams Eldin, N.M., and Emaraa, I. (2017). Arginase enzyme activity and lactoferrin protein concentration in egyptian diabetic patients. Int. J. Adv. Res. (Indore) *5*, 1518–1523.

84. Velnar, T., and Gradisnik, L. (2018). Tissue Augmentation in Wound Healing: the Role of Endothelial and Epithelial Cells. Med. Arch *72*, 444–448.

85. Bao, P., Kodra, A., Tomic-Canic, M., Golinko, M.S., Ehrlich, H.P., and Brem, H. (2009). The Role of Vascular Endothelial Growth Factor in Wound Healing. J. Surg. Res *153*, 347–358.

86. Morgan, C., and Nigam, Y. (2013). Naturally derived factors and their role in the promotion of angiogenesis for the healing of chronic wounds. Angiogenesis *16*, 493–502.

87. Johnson, K.E., and Wilgus, T.A. (2014). Vascular Endothelial Growth Factor and Angiogenesis in the Regulation of Cutaneous Wound Repair. Adv. Wound Care (New Rochelle) *3*, 647–661.

88. Sorg, H., Tilkorn, D.J., Hager, S., Hauser, J., and Mirastschijski, U. (2017). Skin Wound Healing: An Update on the Current Knowledge and Concepts. Eur. Surg. Res. *58*, 81–94.

89. Seitz, O., Schürmann, C., Hermes, N., Müller, E., Pfeilschifter, J., Frank, S., and Goren, I. (2010). Wound healing in mice with high-fat diet- or ob gene-induced diabetes-obesity syndromes: a comparative study. Exp. Diabetes Res. *2010*, 476969.

90. Pereira da Silva, L., Neves, B.M., Moura, L., Cruz, M.T., and Carvalho, E. (2014). Neurotensin Decreases the Proinflammatory Status of Human Skin Fibroblasts and Increases Epidermal Growth Factor Expression. Int. J. Inflam *2014*, 248240.

91. Yamaguchi, M., Matsuura, M., Kobayashi, K., Sasaki, H., Yajima, T., and Kuwata, T. (2001). Lactoferrin protects against development of hepatitis caused by sensitization of Kupffer cells by lipopolysaccharide. Clin. Diagn. Lab. Immunol. *8*, 1234–1239.

92. Boukamp, P., Petrussevska, R.T., Breitkreutz, D., Hornung, J., Markham, A., and Fusenig, N.E. (1988). Normal keratinization in a spontaneously immortalized aneuploid human keratinocyte cell line. J. Cell Biol. *106*, 761–771.

93. Mouritzen, M.V., and Jenssen, H. (2018). Optimized Scratch assay for in vitro testing of cell migration with an automated optical microscope. J. Vis. Exp. *138*, 57691.

94. An, Q., Han, C., Zhou, Y., Li, F., Li, D., Zhang, X., Yu, Z., Duan, Z., and Kan, Q. (2015). In vitro effects of mitomycin C on the proliferation of the non-small-cell lung cancer line A549. Int. J. Clin. Exp. Med. *8*, 20516–20523.

95. Mouritzen, M.V., Abourayale, S., Ejaz, R., Ardon, C.B., Carvalho, E., Dalgaard, L.T., Roursgaard, M., and Jenssen, H. (2018). Neurotensin, substance P, and insulin enhance cell migration. J. Pept. Sci *24*, e3093.

96. Lin, P., Lan, X., Chen, F., Yang, Y., Jin, Y., and Wang, A. (2013). Reference gene selection for real-time quantitative PCR analysis of the mouse uterus in the peri-implantation period. PLoS ONE *8*, e62462.

97. Schmittgen, T.D., and Livak, K.J. (2008). Analyzing real-time PCR data by the comparative C(T) method. Nat. Protoc. *3*, 1101–1108.

98. Mouritzen, M.V., Andrea, A., Qvist, K., Poulsen, S.S., and Jenssen, H. (2019). Immunomodulatory potential of Nisin A with application in wound healing. Wound Repair Regen. *27*, 650–660.

99. Yang, Q., Phillips, P.L., Sampson, E.M., Progulske-Fox, A., Jin, S., Antonelli, P., and Schultz, G.S. (2013). Development of a novel ex vivo porcine skin explant model for the assessment of mature bacterial biofilms. Wound Repair Regen. *21*, 704–714.

100. Moura, L.I.F., Dias, A.M.A., Leal, E.C., Carvalho, L., de Sousa, H.C., and Carvalho, E. (2014). Chitosan-based dressings loaded with neurotensin–an efficient strategy to improve early diabetic wound healing. Acta Biomater. *10*, 843–857.

101. Steinstraesser, L., Hirsch, T., Schulte, M., Kueckelhaus, M., Jacobsen, F., Mersch, E.A., Stricker, I., Afacan, N., Jenssen, H., Hancock, R.E.W., and Kindrachuk, J. (2012). Innate defense regulator peptide 1018 in wound healing and wound infection. PLoS ONE *7*, e39373.

102. Han, H.W., Chang, H.C., Hunag, A.H., and Chang, T.C. (2015). Optimization of the score cutoff value for routine identification of Staphylococcus species by matrix-assisted laser desorption ionization-time-of-flight mass spectrometry. Diagn. Microbiol. Infect. Dis. *83*, 349–354.

103. Moura, J., Sørensen, A., Leal, E.C., Svendsen, R., Carvalho, L., Willemoes, R.J., Jørgensen, P.T., Jenssen, H., Wengel, J., Dalgaard, L.T., and Carvalho, E. (2019). microRNA-155 inhibition restores Fibroblast Growth Factor 7 expression in diabetic skin and decreases wound inflammation. Sci. Rep. *9*, 5836.

104. Tellechea, A., Leal, E.C., Kafanas, A., Auster, M.E., Kuchibhotla, S., Ostrovsky, Y., Tecilazich, F., Baltzis, D., Zheng, Y., Carvalho, E., et al. (2016). Mast cells regulate wound healing in diabetes. Diabetes *65*, 2006–2019.

105. Ukong, S., Ampawong, S., and Kengkoom, K. (2008). Collagen Measurement and Staining Pattern of Wound Healing Comparison with Fixations and Stains. J. Microsc. Soc. Thai. *22*, 37–41.